An ultra miniaturized high data rate MIMO antenna for wireless implantable medical application

BALU ASHVANTH*
Dept. of ECE, Vel Tech Rangarajan Dr. Sagunthala R&D Institute of Science and Technology, Chennai-62, India

A compact Multiple input multiple output (MIMO) antenna is designed and investigated for increasing the transmission data rate and minimizing the multipath fading in implantable biomedical applications. The proposed antenna has an overall dimension of $\pi \times 6.5^2 \times 0.635 mm^3$ and uses an RT3010 substrate of thickness 0.635mm. The newly designed antenna elements adopt two zigzag structures in every antenna element, one with patch interconnection while the other acts as a virtual ground. The zig zag structure in the ground layer improves the gain to -25.2dB, which is reasonably high among this kind of compact four element MIMO antenna. Both of them are coupled together through metallic via to lower the resonant frequency to 430MHz covers the Medical Implant Communication Services (MICS) band of 402–405MHz. The horizontal slots in the patch and "T" slots in the ground plane are etched to reduce mutual coupling among the feeding ports. The antenna is optimized to cover the frequency range 370MHz to 540MHz with a -10dB fractional bandwidth of 37.74%. Simulation in a skin phantom provides better impedance matching and mutual coupling of less than -20dB in the operating band. The simulation results are validated by the measurement carried over with an antenna inserted in a solution. The measurements are in good accordance with simulation results.

(Received September 28, 2023; accepted July 30, 2024)

Keywords: MIMO Antenna, Biomedical applications, MICS band, Miniaturized antenna

1. Introduction

The increasing rate of production of tiny implantable devices for continuous monitoring of patients in the medical field influences the demand for compact antenna to be used in the device. In the research work reported in [1], a meander line has been included inside the asymmetrical U-shaped structure to increase the electrical length of the antenna without increasing its mechanical dimensions. The use of a meandered line reduces the resonant frequency to 915MHz. However, it was a single-element antenna and realized a lower bandwidth of 18.9%.

A dual-element implantable MIMO antenna was designed in the work [2] to support high-data-rate communication and sense pathological changes inside the GI tract. The compactness of the design was achieved using multiple slots in the patch, shorting pins, and high-permittivity substrate. However, it resonates at 915 MHz with a fractional bandwidth of 6.95% and isolation of around 21 dB. The electrically small antenna proposed in [3] utilizes a receded ground plane along with meandered patch to improve its gain performance and achieve resonance, at the desired sub-GHz design frequency of 915 MHz. A dipole antenna in [4] utilizes a helical structure to lengthen the current route of the dipole for size reduction and applies the magnetic sheet with high permeability to shrink the effective wavelength and enhance the radiation efficiency. However, in the above research articles, the antenna was in a rectangular shape which may cause some damage to the human tissue and its operational bandwidth is very narrow. The antenna reported in [5] adopts two planar helical radiators to achieve size miniaturization. Some I-type patches are located between two radiators and slotting structures on the ground plane to reduce coupling. However, it uses a folded metal plate as a radiator, hence care must be taken while implanting in the human tissue and this technique provides less miniaturization. A four element MIMO antenna is reported in [6, 7] to achieve high data rate with reduced multipath effect. The EBG based radiator is adopted to realize miniaturization and also for reducing mutual coupling among the antenna elements. However the attained gain is only -28dBi. A two element MIMO antenna made up of thin substrate is illustrated in [8, 9, 10] for capsule endoscopy application. The step patch along with ground slot produces orthogonal polarization among the antenna elements and this reduces the mutual coupling to -40dB. However the antenna is bent for placing inside the capsule. An electrically small 2×2 MIMO antenna with meandered resonators was demonstrated in the article [11]. Here the meandered line brings size miniaturization and the mutual coupling was minimized using ground slots. Sometimes it is necessary for an antenna to support multiple services and hence it requires wide bandwidth. Among the available methods, the double metallic layers [12] and defective ground [13, 14] methods are more suitable to be used in implantable antennas without increasing their profile size. However, directly exposing the human tissue to the metallic layer (Metallic layer above the superstrate) is not recommended in implantable applications. In this article, a MIMO antenna with four antenna elements is designed for patient health monitoring in biomedical applications. The miniaturization of antenna size is achieved by coupling of patch to the virtual ground through metallic via. The manuscript is organized as follows: Section II describes the antenna geometry and its various stages of evolution is

elaborated in Section III. The reflection coefficients and radiation pattern realized by the antenna are analyzed deeply in Section IV followed by concluding remarks in Section V

2. Antenna geometry

First and foremost, in the antenna design is to decide its size and shape according to the intended application. Based on this, the size of the antenna is planned to be circular to avoid any tissue damage by sharp edges. The diameter of an antenna is optimized to be 13mm. Fig. 1 shows the geometry of the proposed implantable antenna mounted on a grounded Rogers RO3010 substrate with a dielectric constant of 10.2 and a loss tangent of 0.0035. To improve the transmission capacity and alleviate multipath fading phenomena, the MIMO technique is used which accommodated four antenna elements respectively positioned in each quadrant. In addition, the larger the transmission range, the lesser the operating frequency. Thus, from the three MICS bands, the lower (402-405MHz) band has been chosen. To attain this lowest resonant frequency, a zigzag structure is adopted in each antenna element which increases the electrical length of an antenna. An identical zigzag structure is employed as a virtual patch at the bottom of the substrate. Both the zig-zag structures are interconnected through metallic vias for realizing further miniaturization. The common circular ground in the middle has four coaxial feeds that excite four individual patches at the top. The hammer-shaped slots at the ground in between feeds improve isolation among antenna elements. The whole design is preceded by a superstrate made of Rogers RO3010. In the proposed antenna, zigzag structure is employed which brings multiple phase shifts to the current flowing through it and increases the electrical length of an antenna. Hence reduces the resonant frequency by multifold. The antennas zigzag length is increased to L=43mm to bring down the resonant frequency to 430MHz. The radius of an antenna is optimized to 6.5mm to accommodate this zig-zag structure.

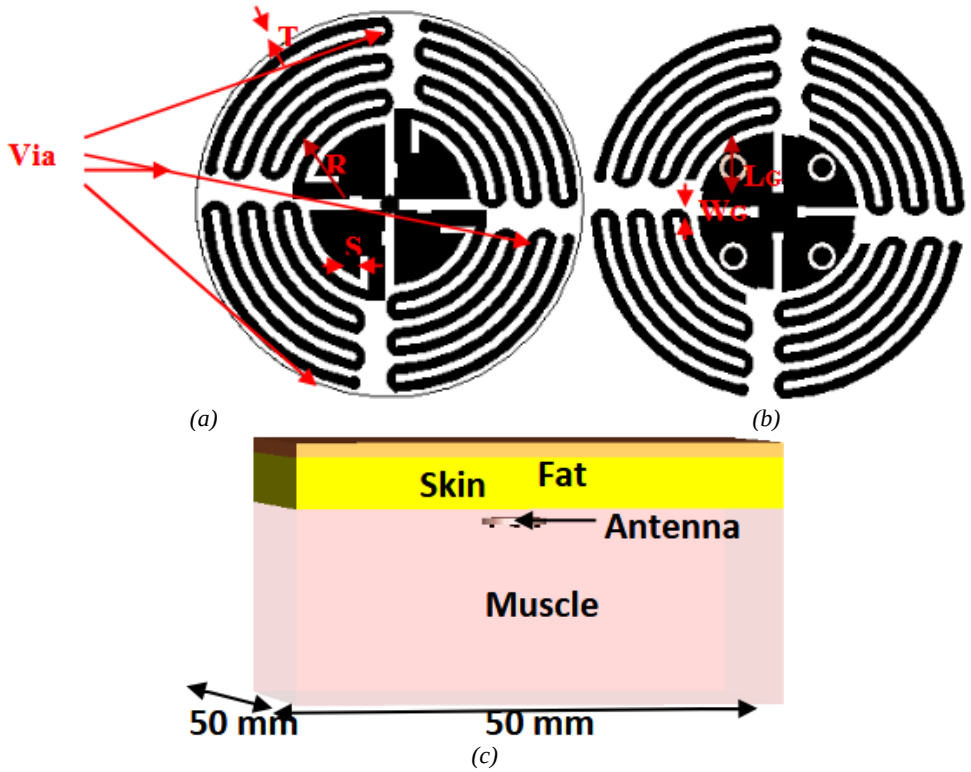

Fig. 1. Geometry of the Proposed Antenna (a) Front view, (b) Rear view, (c) Simulation model (color online)

To approximate more closely to the real human body and save computing time, a three-layer phantom is adopted in the simulation. Fig. 1(c) shows the scenario of implanting the proposed antenna in a multilayer tissue phantom which is composed of skin, fat, and muscle to imitate the real situation inside the human body. The skin thickness is 1.5mm with relative permittivity, and conductivity of 52.7 and 1.46 respectively. The second layer is made up of fat having a thickness of 10.5mm with permittivity, and conductivity of 5.28 and 0.10 respectively. The bottom layer is composed of muscle with 40mm thickness and has relative permittivity, and conductivity of 38 and 1.71 respectively. The antenna is placed in the muscle at a depth of 4mm from the fat. The antenna zigzags meandered line length is L=43mm and other dimensions are Lc= 2.5mm, Wc= 0.4mm, R= 2.5mm, T= 0.3mm, S= 0.4mm. The relative permittivity of the substrate material is one of the variables that affects how compact an antenna is. The antenna is more compact the higher the permittivity. The isolation between the

antenna elements in a MIMO antenna design is determined by the substrate's thickness. High isolation is achieved by limiting surface waves between antenna elements by using an ultrathin substrate. For the patch and ground, conductor materials like copper, silver, and gold are advised. Copper has been employed in the proposed antenna to lower the cost of manufacture.

3. Evolution

The desired results of the designed antenna are obtained in three iterative steps, as shown in Fig. 2. It is worth noting that the antenna in stage 1 has a circular patch that is bisected into four quadrants by a plus-shaped slot with a complete ground at the bottom. On exciting each quadrant with a coaxial feed provides resonance at 1.29GHz. The initial patch dimension is calculated using

$$f = \frac{1.8412 \times C}{8\pi R\sqrt{\varepsilon_r}}$$

where C is the velocity of light, R is the radius of the patch, ε_r is the relative permittivity of the substrate, f is the resonant frequency.

$$V_p = \frac{1}{\sqrt{L\,C}} = \lambda_g f$$

The patch is modified in stage 2 by including a zig-zag structure that operates at 1.15GHz. The inclusion of the zig-zag structure provides a parallel combination of capacitance and inductance, hence total inductive capacitance effect increases in the antenna which brings down the frequency. In stage 3, the radius of the circular patch is reduced to 4.3mm and it is extended with a zig-zag structure having two bends. A similar zig zag shape is attached to the ground and it is interconnected to its counterpart at the top layer by vias which renders resonance at 554MHz. for achieving further miniaturization, the length of the zig-zag structure is increased from 27mm to 43mm and thus the operating frequency is reduced to 430MHz as depicted by stage 4 of Fig. 2. By properly positioning the coaxial feed and disconnecting center slotted ground from the surrounding zig-zag structure, a better impedance matching, improved isolation along with reduced return loss are obtained.

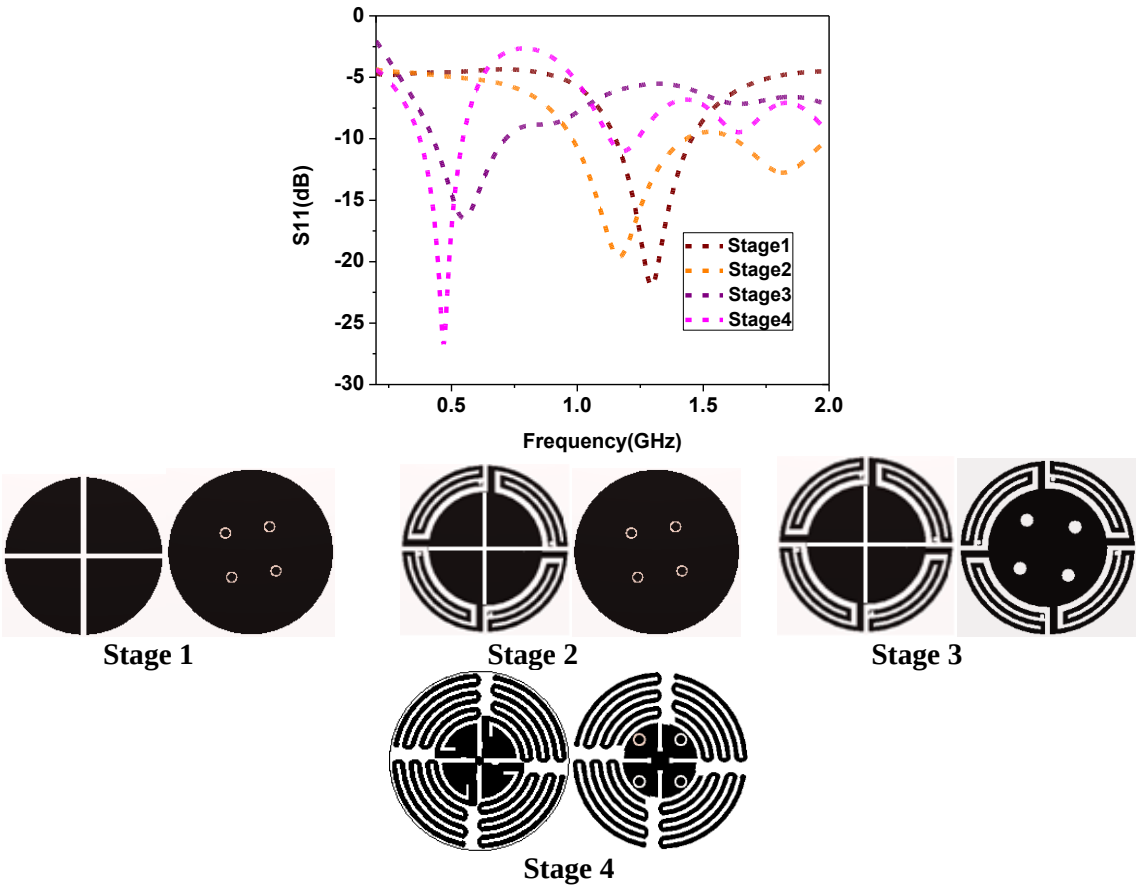

Fig. 2. Reflection coefficients during the evolution of the proposed antenna (color online)

Stage 2 of Fig. 2 illustrates how the addition of the Electromagnetic band-gap (EBG) structure results in a parallel combination of capacitance and inductance, increasing the antenna's overall inductive capacitance impact and lowering the frequency. While Artificial Magnetic Conductors (AMC) when integrated into an antenna improves antenna performance like gain, bandwidth, multiband characteristics, radiation properties, beamwidth, polarization, impedance etc., along with bandgap, Electromagnetic band-gap (EBG) is a Periodic structure that passes certain frequency bands, rejects some frequency bands, and thus renders the band gap or mirror in the operational bandwidth along with bandwidth enhancement. The zig-zag structure in our research provides a stop band, which lessens mutual coupling between the antenna elements in the operational band and offers a broader bandwidth; as a result, it is recognized as EBG.

4. Results and discussion

Fig. 3 shows the effect on the reflection coefficient while changing the zigzag dimensions. The first parameter is the length of the zigzag structure. Its effect is plotted in Fig. 3 (a) for different lengths of 12mm, 27mm, and 33mm. It can be seen that the center frequency shifts from 465MHz to 911MHz and thus the length has a major impact on the operating frequency of the proposed antenna. The second parameter to be analyzed is the thickness of the zigzag meandered line (T). A variation between 0.2 and 0.4 mm has been considered. It is inferred that an increase in the thickness increases the resonant frequency from 410MHz to 515MHz, as shown in Fig. 3 (b). It can be appreciated that the optimized values (L=43mm, T=0.3mm) provide better impedance matching with reduced return loss.

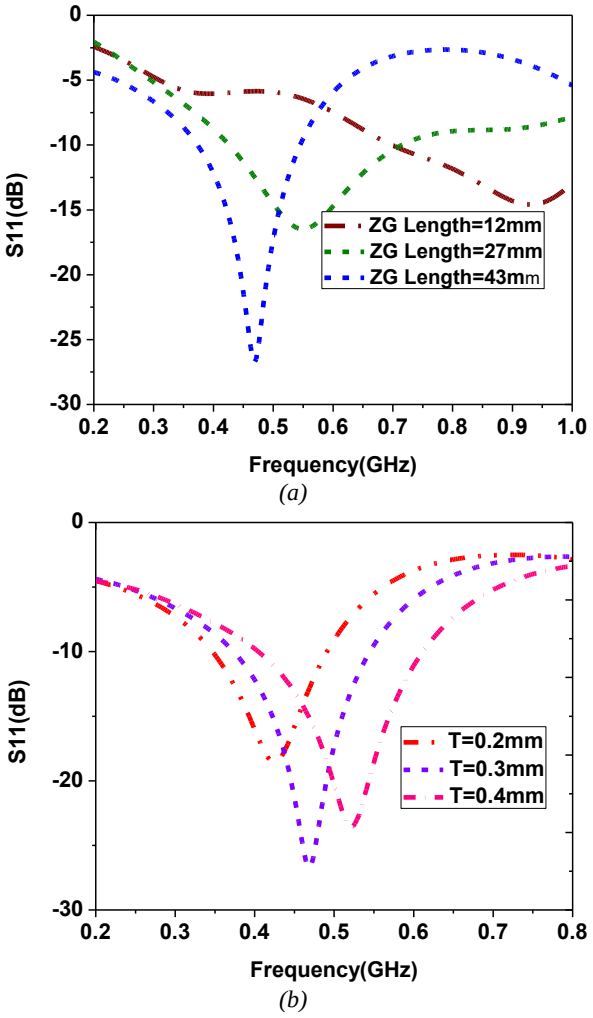

Fig. 3. Parametric analysis of implantable MIMO antenna by varying (a) zigzag length, (b) zigzag thickness (color online)

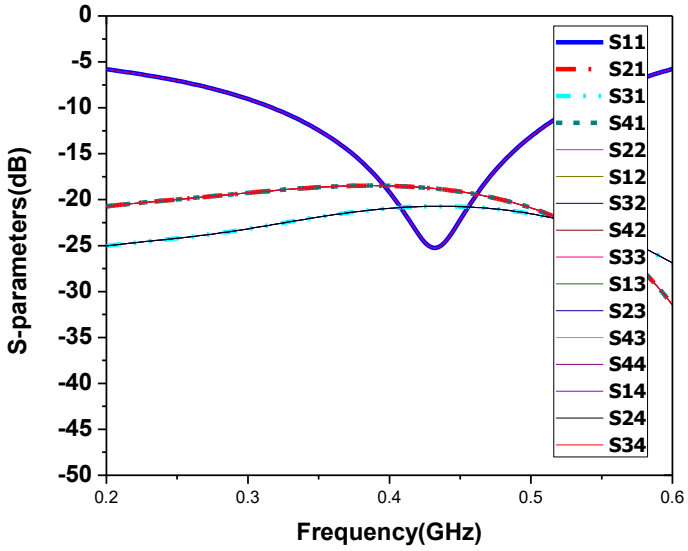

Fig. 4. S-parameters of the proposed antenna (color online)

The important factors to be considered for the MIMO antenna are return loss and mutual coupling. It has been observed from Fig. 4 that the transmission coefficients (S21, S31, S41, S12, S32, S42, S13, S23, S43, S14, S24, S34) are closer to -20dB, and thus reduced mutual coupling is ensured between the four ports when all of them are excited instantaneously. As illustrated in Fig. 4, the reflection coefficient is less than -25dB at the operating frequency of 430MHz which assures the minimum return loss at the feeding port.

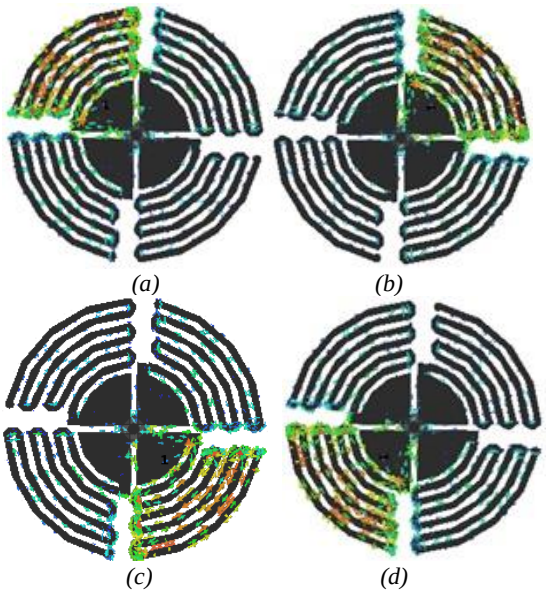

Fig. 5. Surface current distribution on exciting (a) port1, (b) port 2, (c) port 3, (d) port 4 (color online)

The study of surface current distribution is done to understand the coupling intensity phenomenon between the antenna elements. The zigzag structure acting as electromagnetic bandgap (EBG) and ground slots prevent electromagnetic energy coupling between antenna elements. Finally, the current is trapped in the zigzag structure, as shown in Fig. 5, which significantly improves the isolation between the antenna elements. When port 1 is excited, the surface current concentration is more on the EBG structure of the patch associated with port 1. It can be seen that only a small amount of current couples with adjacent elements and negligible current coupling with other antenna elements. Thus, the current level in the exciting element is higher than the non-excited element even with a smaller separation distance. Furthermore, the current intensity on the ground plane below the excited port is higher than the other part of the ground plane, which further confirms weak coupling between the radiators.

A microstrip patch antenna must be fabricated in a few steps. They are outlined below:

1. Transparency film is created as the initial step in the production process, and the patch and ground structures of an antenna are printed on it.

2. In the UV exposure machine, the transparency film is affixed to both sides of copper-coated dielectric material and exposed to ultraviolet radiation.

3. The photolithographic process etches away the copper that is exposed to the UV on each side of the substrate. The undesired metal portions of the metallic layer are removed by the chemical etching process used in the photo-lithographic procedure. The microstrip patch's highly precise etched pattern is created using the photolithographic process.

4. Attach the feed: A coaxial cable is normally used to connect the feed point. Soldering or employing conductive adhesive can be used for this.

5. Test the antenna: Lastly, to make sure the antenna is functioning properly, it should be tested. An analyzer for vector networks can be used for this. By positioning the constructed antenna as the receiving antenna above the rotatable stand in an anechoic room and the horn as the sending antenna, radiation patterns may be monitored. The E plane and H plane patterns were created by rotating the antenna in the azimuth and elevation planes, and the VNA has shown these patterns.

Fig. 6 shows the comparison of the simulated and measured reflection coefficients. Even though the measured S11 < -10 dB bandwidth is narrower than the simulated results, it covers the MICS band of 433MHz. The human muscle equivalent solution is used for S11 and radiation pattern measurement whose ingredients are distilled water and sugar mixed in 3:2 proportions. Using the "keysight materials measurement suite" software that is loaded on a computer, the relative permittivity of the liquid is determined. This measurement uses an adapted version of the coaxial probe method. This method involves connecting an electrode submerged in distilled water to the computer via a coaxial connection. At first, distilled water by itself was tested and found to have a dielectric constant of 78.4. After that, the sugar was increased little by little until the two-dimensional display curve reached 38, the necessary dielectric constant value for replacing human tissue. For the needed relative permittivity, it was determined that 50% of the liquid's sugar content was present.

(a)

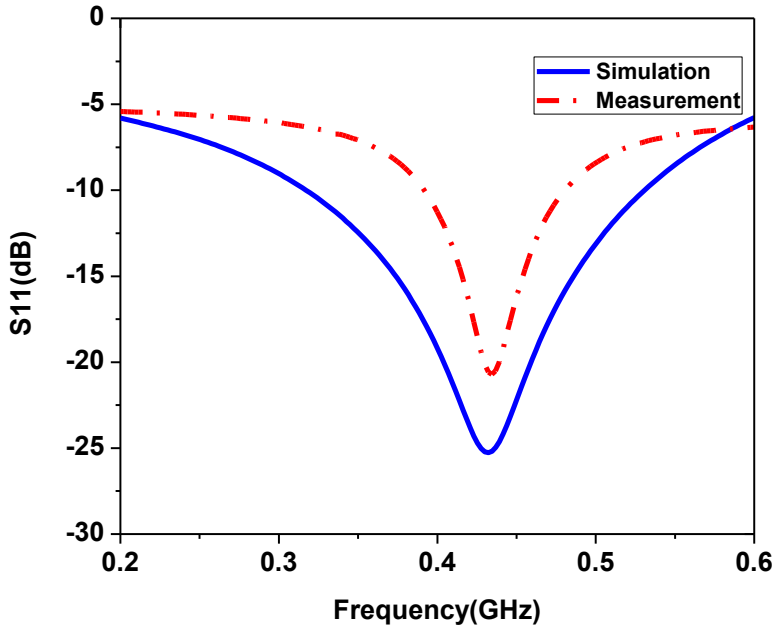

(b)

Fig. 6. (a) Fabricated antenna &measurement setup, (b) Simulation and measurement S11 comparison (color online)

Fig. 7 illustrates the comparison of simulated and measured radiation patterns. The measurement was taken in an anechoic chamber by immersing AUT in the prepared solution while the horn on the other side acted as a reference antenna.

The comparison of the proposed work with similar research works involving the design of implantable MIMO antennae for biomedical applications is shown in Table 1. It is observed that the proposed four-element implantable MIMO antenna operates at 460MHz which covers the ISM band of 403MHz. This is the lowest operating band having wider bandwidth than similar implantable MIMO antenna works. In addition, the proposed antenna achieves better miniaturization than similar works reported. In this work, a circular shape is adopted for the antenna structure to avoid causing any damage to the tissues surrounding it, while other works used square or rectangular shapes. A reasonable gain is realized with the reported antenna which is high when compared to most of the related works. The maximum input power to the proposed antenna should be less than or equal to 4.8mW for satisfying the Specific Absorption Rate (SAR) given by the IEEE guidelines for human safety. The proposed implantable MIMO antenna exhibits a radiation efficiency of 0.21%

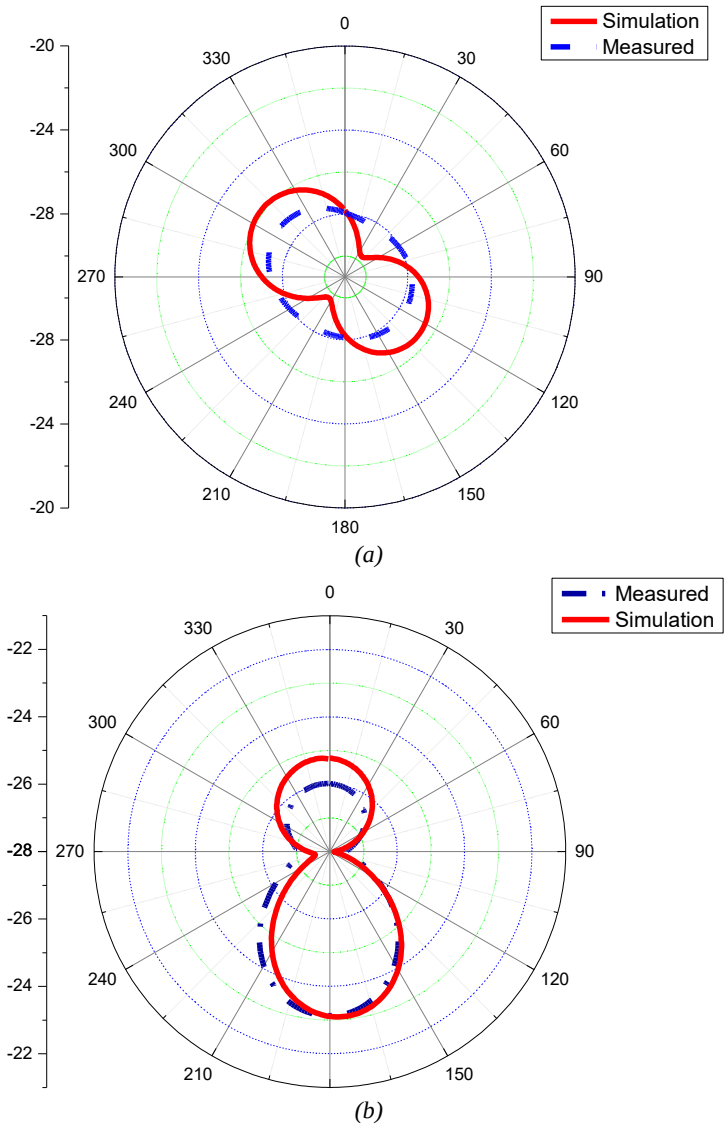

Fig. 7. Radiation pattern at 403MHz in (a) E plane view, (b) H plane view (color online)

Table 1. Comparison of proposed work with similar research works

Ref	No. of Elements	Size (mm^3)	ISM Band	Bandwidth	Gain	Techniques
[2]	2	$\pi \times 6^2 \times 0.13$	915MHz	6.95%	-32dB	Slotted patch
[3]	1	12.75×12.25×0.29	915MHz	2.82%	-19.88dB	Meandered line
[7]	4	18.5×18.5×1.27	2.45GHz	18.64%	-15.2dB	Cross & EBG slots to improve isolation
[8]	4	13.5×13.5×0.13	433MHz	38.26%	-28dB	Semicircular strip-based patch, Via
This work	4	$\pi \times 6.5^2 \times 0.63$	403MHz,	37.74%.	-25.2dB	Circular shape, EBG structure, Slots, Via

5. Conclusion

A compact MIMO antenna was designed and tested for implantable biomedical applications. It resonates at 460MHz which covers the ISM band of 403MHz with an operational bandwidth of 37.74%. Interconnection of zigzag structures at the patch and ground through metallic via provided the size miniaturization. The mutual coupling among the antenna elements was reduced by etching four bisecting slots at the ground and patch. The zigzag

structure of the patch acted as an AMC and thus rendered resonance as well as a band gap. The antenna realized a better gain of -25.2dB by the adopted structure. The simulated results were validated with the measurement results. The high data rate supporting capability of this antenna makes it a suitable candidate for live surgeries and other biomedical applications

References

[1] Abdenasser Lamkaddem, Ahmed El Yousfi, Kerlos Atia Abdalmalak, Vicente González Posadas, Daniel Segovia-Vargas, IEEE Transactions on Antennas and Propagation **70**(8), 6423 (2022).
[2] Amjad Iqbal, Muath Al-Hasan, Ismail Ben Mabrouk, Tayeb A. Denidni, IEEE Sens. J. **23**(3), 2105 (2023).
[3] Andrew J. Mugisha, Amin Rigi, Andreas Tsiamis, Symon Podilchak, Srinjoy Mitra, IEEE J. Rad. Freq. Ident. **40**(4), 2210 (2023).
[4] Xiao Fang, Xufeng Du, Michael Bärhold, Qiong Wang, Dirk Plettemeier, IEEE Antennas and Wireless Propagation Letters **21**(12), 2502 (2022).
[5] Kuo Liu, Ziwei Li, Wenjie Cui, Kanglong Zhang, Mengjun Wang, Chao Fan, Hongxing Zheng, Erping Li, IEEE Trans. Ant. Propag. **70**(12), 11324 (2022)
[6] Yi Fan, Jinhong Huang, Tianhai Chang, Xiong Ying Liu, IEEE J. Electromagn. RF Microw. Med. Biol. **2**, 4 (2018).
[7] Amjad Iqbal, Muath Al-Hasan, Ismail Ben Mabrouk, Mourad Nedil, IEEE Antennas and Wireless Propagation Letters **25**, 5 (2021).
[8] Rongqiang Li, Yongxin Guo, IEEE Antennas and Wireless Propagation Letters **20**, 4 (2021).
[9] Xin Yang, Xian Qi Lin, BaoWang, Yihong Su, IEEE Transactions on Antennas and Propagation **69**, 7 (2021).
[10] Moirangthem Santoshkumar Singh, Jeet Ghosh, Soumendu Ghosh, Abhishek Sarkhel, IEEE Antennas and Wireless Propagation Letters **20**; 8 (2021).
[11] Abdullah J. Alazemi Member, Amjad Iqbal, IEEE Transactions on Antennas and Propagation **1**, 1 (2021).
[12] Daibin Jing, Hua Li, Xiao Ding, Wei Shao, Shaoqiu Xiao, IEEE Antennas and Wireless Propagation Letters **5**, 1 (2023).
[13] Naeem Abbas, Syed Ahson Ali Shah, Abdul Basir, Zubair Bashir, Adeel Akram, Hyoungsuk Yoo, IEEE Access **10**, 66018 (2022).
[14] Farooq Faisal, Muhammad Zada, Hyoungsuk Yoo, Ismail Ben Mabrouk, Mohamed Chaker, Tarek Djerafi, IEEE Transactions on Antennas and Propagation **70**(7), 5923 (2022).

*Corresponding author: drashvanthb@veltech.edu.in